

## Article

# Spatiotemporal Evolution of Land Cover and Landscape Ecological Risk in Wuyishan National Park and Surrounding Areas

Yuzhi Liu <sup>1</sup>, Wenping Cao <sup>2,\*</sup>  and Fuyuan Wang <sup>3,4,\*</sup>

<sup>1</sup> School of Soil and Water Conservation, Beijing Forestry University, Beijing 100083, China; liuyuzhi627@bjfu.edu.cn

<sup>2</sup> College of Tourism Management, Hunan Vocational College of Commerce, Changsha 410205, China

<sup>3</sup> Institute of Geographic Sciences and Natural Resources Research, Chinese Academy of Sciences, Beijing 100101, China

<sup>4</sup> Key Laboratory of Regional Sustainable Development Modeling, Chinese Academy of Sciences, Beijing 100101, China

\* Correspondence: caowenping@hnrcc.edu.cn (W.C.); wangfy@igsnr.ac.cn (F.W.)

**Abstract:** Previous research on national park conservation has predominantly concentrated on their internal regions, with scant attention given to the parks and their adjacent areas as integrated entities. Therefore, the investigation of land cover and landscape ecological risks in national parks and surrounding areas is essential for overall ecosystem protection and regional sustainable development. This study examines the spatiotemporal evolution of land cover and its landscape ecological risk in Wuyishan National Park, China, and its surrounding areas (WNPSA) from 1990 to 2020. The results show that (1) the land cover of WNPSA from 1990 to 2020 predominantly exhibited a consistent decline in forested areas, paralleled by an augmentation in farmland and impervious surface areas. The center of standard deviation ellipse of impervious surfaces has been progressively moving further south in tandem with the expansion of these surfaces, primarily located within the county town of Fujian Province. (2) The Wuyishan National Park (WNP) areas were dominated by low values of landscape index, and the high value areas in the park were mainly located at the provincial boundary area, with a gradual narrowing during 1990–2020, suggesting a decrease in landscape heterogeneity within the park. High value areas in the surrounding areas mainly occurred in areas with clustered impervious surfaces (e.g., the county town), where part of them located in Wuyishan City have spread to the edge area southeast of WNP. (3) From 1990 to 2020, the lowest-risk areas continue to expand. However, as the medium-risk zone of the adjacent region extends into the edge of the national park, the low risk zone within the national park exhibits a trend from continuous to separate with the neighboring low risk zone. This led to an escalating stress effect on the ecological security of both the adjacent regions and the national park's boundary areas due to land cover changes.

**Keywords:** national park; Wuyishan National Park; land cover change; spatiotemporal evolution; landscape pattern index; landscape ecological risk



**Citation:** Liu, Y.; Cao, W.; Wang, F. Spatiotemporal Evolution of Land Cover and Landscape Ecological Risk in Wuyishan National Park and Surrounding Areas. *Land* **2024**, *13*, 646. <https://doi.org/10.3390/land13050646>

Academic Editors: Benjamin Burkhard and Javier Martínez-López

Received: 16 March 2024

Revised: 30 April 2024

Accepted: 3 May 2024

Published: 9 May 2024



**Copyright:** © 2024 by the authors. Licensee MDPI, Basel, Switzerland. This article is an open access article distributed under the terms and conditions of the Creative Commons Attribution (CC BY) license (<https://creativecommons.org/licenses/by/4.0/>).

## 1. Introduction

National parks play a pivotal role in promoting ecological environment protection and are essential for effectively preserving biodiversity and mitigating global climate change [1,2]. Following the 1870s, the concept and establishment of national parks underwent a global expansion from the United States. This led to the formation of representative national park development models such as the American wilderness model, the European model, the Australian model, and the British model [3]. The “surrounding area” pertains to the region adjacent to a national park. It serves as the primary hub for tourism services and plays a crucial role in regional ecological network protection and socio-economic development [4].

In the context of China's rapid urbanization, the rapid development of urbanization in areas surrounding some nature reserves has led to a significant expansion of impervious surfaces in villages and towns and to the proximity of the edges of some nature reserves, ultimately creating ecological risks to regional landscapes [5]. Consequently, investigating the spatiotemporal evolution of land use/cover and its associated landscape ecological risk in national parks and their vicinities is vital for comprehending shifts in the ecological environment both inside and around these parks, as well as for ensuring regional ecological security. WNP is one of the first five national parks to be officially established in China in 2021, and it is also one of the national parks with the most frequent human activities [6], so it is representative to select it as a research object.

National parks, a significant type of nature reserves, have been the subject of extensive scholarly research. This research has explored various fields such as the ecological safety and quality [7–9] of national parks or nature reserves, specific resource types or land classes [10–12], ecological protection compensation or immigration [13,14], community conflicts [15], and their impact on physical and mental health [16]. The perspective of this research has evolved from a purely "biocentrism" concept to an increasing appreciation for the interaction process between national parks and multiple stakeholders [17]. Among these, landscape and land use/cover and ecosystem protection have consistently been focal points in national park research. Relevant studies have identified ecological risks within national parks due to factors such as unreasonable development, excessive resource utilization, human activity interference, and extreme natural disaster events. These factors have led to significant changes in the land cover of nature reserves, with issues such as forest and grass degradation [18–20], wetland loss [21,22], and landscape fragmentation [23,24] continuously emerging. Some studies have indicated that the vegetation coverage of China's five major national parks all displayed a fluctuating upward trend from 2000 to 2020. In particular, the Northeast Tiger Leopard National Park exhibited the most pronounced vegetation reduction trend [25], with higher and highly fragmented areas accounting for 8.96% of the park's total area, primarily located in population concentration areas [26]. In the case of the Hainan tropical rainforest national park, cultivated land, grassland, and natural forest decreased by 68.48%, 18.74%, and 4.89%, respectively, from 1990 to 2018 [27]. However, after the completion of a highway in 2019, there was an increase in forest area and forest patch density, but an intensification of fragmentation [28]. Three types of land, desert, grassland, and water were converted to each other during the period 2000–2020 in Sanjiangyuan National Park, and the larger the span of land use transformation, the greater the impact on the value of ecosystem services [29]. In the Simien Mountains National Park, Australia, there was a significant increase in shrub cover by 110.8% (79 ha/year) between 1985 and 2015. Conversely, forest and grassland cover experienced substantial reductions of approximately 56.4% (98 ha/year) and 49% (142 ha/year), respectively [30]. In HNP National Park, Bangladesh, there were notable shifts in land use from 1997 to 2017. This included a degradation trend in dense forests, deterioration in agricultural lands, and an expansion of sparse forests and water. It is projected that these changes in land vegetation will persist over the forthcoming two decades [31]. The establishment and effective management of nature reserves can enhance natural vegetation coverage and improve both the local ecological environment quality and the aesthetic appeal of landscapes [32,33]. Furthermore, Yu et al. employed transition matrix analysis and principal component analysis to demonstrate that nature reserves significantly mitigate the loss of Hainan's natural forests [34]. Scharsich observed that the land cover composition of Matobo National Park in Zimbabwe remained largely stable from 1989 to 2014. In contrast, adjacent areas outside the park underwent significant changes, with an approximate 7% increase in forested areas and a marked transformation in public lands, coupled with a reduction in cultivated land [35]. Mingarro et al. demonstrated that European national parks could enhance the natural conditions of their regions within a few years of inception, thereby exerting a positive impact on their surroundings from 1986 to 2018. This naturalization effect is particularly pronounced in the buffer zone of 1 km

within the longest conservation time reserve. Furthermore, the efficacy of reserves exhibits distinct latitudinal zonality variations [36].

In addition, the exploration of ecosystem integrity [37,38] and ecological security [39,40] within national parks or nature reserves is a significant area of interest in academic research. An empirical assessment of conservation efficacy across six national park case sites in Canada and South Africa has been undertaken. The findings indicate that while certain parks demonstrate proficiency in addressing priorities derived from conservation monitoring data, a comprehensive analysis of all indicators reveals a decline in the conservation effectiveness rating for each park. Consequently, a systematic methodology is imperative for evaluating conservation effectiveness within national parks [41]. Sanjiangyuan National Park's overall landscape ecological vulnerability is low, indicating a less secure status for its land ecological security. The Yangtze River source park and Lancang River source park primarily exhibit an area level of insecurity, followed by a critical safety level. In the Yellow River source park, the proportion of areas at critical safety and above levels stands at 93.94% [42]. From 1980 to 2020, the habitat quality in the counties and cities surrounding WNP was commendable, exhibiting an overall downward trend with minimal amplitude. The ecological security index of the park and its adjacent areas showed a consistent increase trend overall, albeit with notable regional differences [43]. Concurrently, the ecosystem sensitivity of the protection development belt and its surrounding counties around WNP is weak. Therefore, it is imperative to build a theory of national park ecological security pattern characterized by "two cores, three screens, multiple points, multiple corridors" [44].

Prior research has significantly advanced our understanding of park land use/cover change, ecosystems, and ecological security. However, when considering the spatial scope of the research, the majority of studies have primarily concentrated on the interiors of national parks. A limited number of studies have explored the land use in the surrounding areas of these parks. Yet, there has been a dearth of research into the spatiotemporal variation of landscape ecological risk between national parks and their adjacent regions. In response to this gap, this paper focuses on WNP and five county-level administrative districts within its protective development belt. It examines the spatiotemporal dynamics of land cover changes in both national parks and their neighboring areas, investigates the patterns of land cover type transitions and temporal variations, and assesses the landscape ecological risks associated with ecological land use in these regions. Furthermore, it delves into the spatiotemporal evolution of each landscape index. The findings aim to offer insights and recommendations for enhancing ecological security in national parks and their environs, as well as for the governance and protection of the protective development belt surrounding these parks.

## 2. Study Area

WNP is located in the northern section of Wuyi Mountains at the junction of Jiangxi and Fujian provinces in northwestern Fujian (Figure 1), with a total area of 1280 km<sup>2</sup>. It is a famous scenic tourist area and summer resort in China, and has been designated as both a World Cultural and Natural Heritage Site and a World Biosphere Reserve. WNP is characterized by six distinct levels, extending from the west to the east. These levels are interspersed with a range of geomorphological types, transitioning from the central mountainous regions to the hilly basins. This diverse array of geographical features contributes to the park's rich and varied ecological environments, making it a key region for global biodiversity conservation, which has the most complete, typical, and large-area middle subtropical primary forest ecosystem existing at the same latitude belt in the world. It is one of the 11 key regions for global significance terrestrial biodiversity conservation in China and a typical representative of the geological structure of the eastern Pacific Ring of Asia. The national park conservation and development belt is directly connected to the internal ecosystem of the national park, closely related to human activities, and is a buffer zone for the protection of national parks. It is also a key area that supports the green

development of national parks and explores the harmonious coexistence between man and nature [44]. In order to expand the scope of national park protection coordination and avoid the isolation of national parks, Nanping City, Fujian Province put forward the idea of building a Wuyishan national park conservation and development belt (excluding the national park), preliminarily delimited the scope of the belt about 4252 km<sup>2</sup>, involving four counties (cities, districts) of Wuyishan, Jianyang, Shaowu, and Guangze. In addition, a master plan is being prepared for the Wuyishan national park conservation and development belt in Jiangxi Province (i.e., Yanshan County). Since counties (cities, districts) are the basic administrative units for economic and social development and ecological protection in China, this study takes the five counties (cities, districts) involved in the Wuyishan national park conservation and development belt as the research scope.

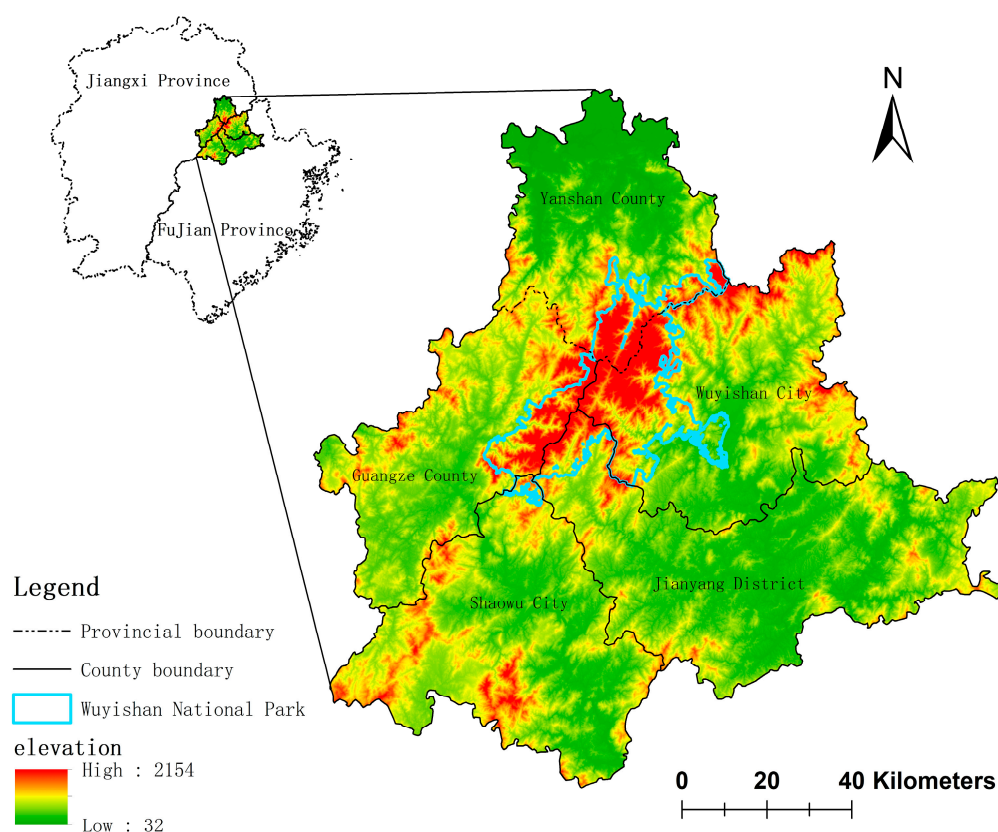


**Figure 1.** Location of WNPSA.

### 3. Data and Methods

#### 3.1. Data Source

The land cover data utilized in this study are derived from the Annual China Land Cover Dataset (CLCD) [45], courtesy of Wuhan University. This dataset spans the years 1985 to 2022, offering a spatial resolution of 30 m. With an overall accuracy of 80%, it satisfies the necessary application criteria. Land cover data for four periods, 1990, 2000, 2010, and 2020, were selected for this study (Figure 2). By aligning with the administrative vector boundaries of the designated WNPSA, seven different land cover classes were isolated: cropland, forest, shrubland, grassland, water, barren, and impervious. It is important to highlight that the bare land category was absent for both the 1990 and 2000 study periods.

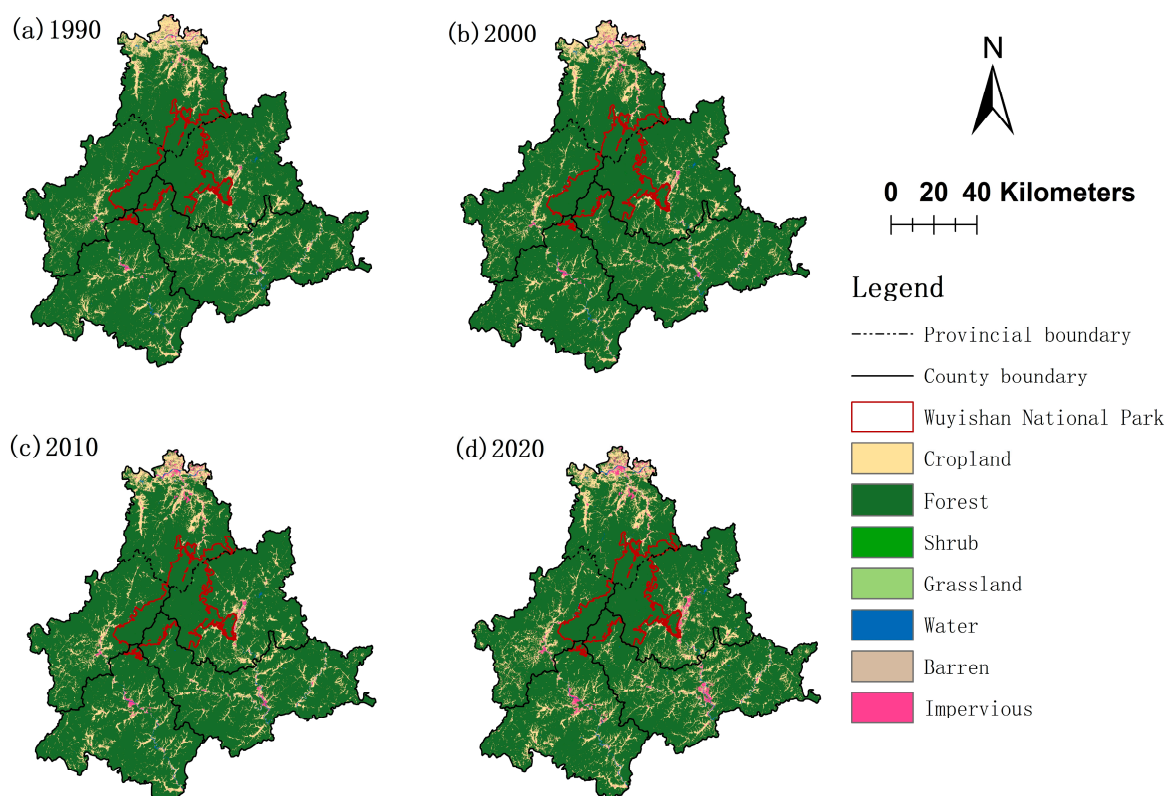


**Figure 2.** Land cover data for WNPSA in 1990 and 2020.

### 3.2. Research Method

#### 3.2.1. Land Cover Transition Matrix

The land cover data of two adjacent periods were overlaid using the Raster Calculator in ArcGIS. The initial and final period's land cover codes served as the tens and units digits, respectively [46], culminating in a two-digit coded land use change map for three distinct periods: 1990–2000, 2000–2010, and 2010–2020. Generated growth and reduce maps [47] were based on the change information across these periods, spatially delineating the transitions in and out of various land cover types. Visualization of the results was obtained from the land cover transfer matrix using the number of transformations between different land cover types, using the land use transfer matrix, and using Sankey diagrams. The formula for land use transition is as follows:

$$X(t+1) = AX(t) \quad (1)$$

In this study,  $X(t)$  denotes the vector of land use conditions for the  $t$ -th period, while  $X(t+1)$  represents the vector of land use conditions for the subsequent  $(t+1)$ -th period. The variable  $A$  is defined as the land use transition matrix. Within this matrix, each row signifies a distinct land use type from one period, whereas each column corresponds to a different land use type in another period. The element  $A(i, j)$  within the matrix symbolizes the probability of transitioning from the land use type in the  $i$ -th period to the corresponding land use type in the  $j$ -th period.

#### 3.2.2. Standard Deviation Ellipse Method

The standard deviation ellipse method is a classical approach for examining the directional characteristics of spatial distribution. This method allows for a quantitative explanation of both global and spatial aspects of feature distribution in terms of centrality, dispersion, directionality, and spatial morphology. In this paper, the standard deviation ellipse method is used to explore the centroid change directions, and dispersion patterns

of land cover types (forest, shrubland, grassland, water), cropland, and impervious surfaces in ecologically classified areas within the Wuyi Mountain region and its surrounding areas over a span of 30 years. The primary parameters of the standard deviation ellipse include the centroid, orientation angle, and major and minor axes, as detailed in Equations (2)–(4) [48]:

$$SDE_x = \sqrt{\frac{\sum_{i=1}^n (x_i - \bar{X})^2}{n}}, SDE_y = \sqrt{\frac{\sum_{i=1}^n (y_i - \bar{Y})^2}{n}} \tag{2}$$

$$\tan \theta = \frac{(\sum_{i=1}^n \tilde{x}_i^2 - \sum_{i=1}^n \tilde{y}_i^2) + \sqrt{(\sum_{i=1}^n \tilde{x}_i^2 - \sum_{i=1}^n \tilde{y}_i^2)^2 + 4(\sum_{i=1}^n \tilde{x}_i \tilde{y}_i)^2}}{2 \sum_{i=1}^n \tilde{x}_i \tilde{y}_i} \tag{3}$$

$$\sigma_x = \sqrt{2} \sqrt{\frac{\sum_{i=1}^n (\tilde{x}_i \cos \theta - \tilde{y}_i \sin \theta)^2}{n}}, \sigma_y = \sqrt{2} \sqrt{\frac{\sum_{i=1}^n (\tilde{x}_i \sin \theta + \tilde{y}_i \cos \theta)^2}{n}} \tag{4}$$

$SDE_x$  and  $SDE_y$  represent the coordinates of the standard deviation ellipse’s centroid.  $x_i$  and  $y_i$  denote the spatial location coordinates of the geographical features.  $\bar{X}$  and  $\bar{Y}$  are the arithmetic centroids of these geographical features, while  $n$  signifies the number of geographical elements. The orientation angle of the ellipse, denoted as  $\theta$ , is defined as the angle between the ellipse’s X-axis and the true north direction ( $^\circ$ ).  $\tilde{x}_i$  and  $\tilde{y}_i$  represent deviations from the mean center. Finally,  $\sigma_x$  and  $\sigma_y$  denote the standard deviations of the X and Y axes, respectively.

### 3.2.3. Land Cover Dynamics

The Land Cover Dynamics model provides a quantitative assessment of the rate at which land cover changes within a given region, and can be bifurcated into two categories: single land cover dynamics and comprehensive land cover dynamics. The former pertains to the rate of change in the area of a specific land use type over a designated time frame, as delineated by Equation (5):

$$K = \frac{S_{t2} - S_{t1}}{S_{t1}} \times \frac{1}{t2 - t1} \times 100\% \tag{5}$$

In this context,  $K$  denotes the dynamics of a specific land cover type over the time span from  $t1$  to  $t2$ . The areas of this particular land cover type during this period are represented by  $S_{t1}$  and  $S_{t2}$ . The variation in the value of  $K$  signifies the quantity of conversion into this particular land cover type. The dynamics of barren cover were not evaluated due to the absence of a barren distribution in both 1990 and 2000, coupled with minimal bare land area observed in 2010 and 2020.

Comprehensive land cover dynamics encapsulate the aggregate rate of land use change across an entire region:

$$S = \left[ \frac{\sum_{j=1}^n \Delta S_{ij}}{2 \sum_{i=1}^m S_i} \right] \times \frac{1}{T} \times 100\% \tag{6}$$

$S$  denotes the comprehensive land use dynamics over a specific time period. The initial area of each land cover type is represented by  $S_i$ , while  $\Delta S_{ij}$  signifies the conversion area from type  $i$  to type  $j$ .  $T$  represents the duration of the research study.

### 3.2.4. Landscape Ecological Risk Model

Landscape loss refers to the extent of loss of natural attributes of ecosystems represented by different landscape types when disturbed by natural and human factors. Landscape disturbance degree and landscape vulnerability are commonly used indices for quantitatively measuring the risk loss of different landscape types. Since this study focuses on the protection of ecosystems in national parks and surrounding areas, and the basis of ecosystem is ecological land, the landscape ecological risk assessment model of ecological land was constructed using landscape disturbance and landscape vulnerability [49], and

spatial visualization was carried out. The calculation of this index also involves landscape fragmentation degree, landscape separation degree, landscape fractal dimension, and other landscape structure indices of ecological land (Table 1) [50–52].

This study utilizes the fishing net analysis function of ArcGIS, adopts the equally spaced grid sampling method, and draws on existing literature to divide WNPSA into 3 km × 3 km grids to obtain 1663 ecological risk sample plots. The ecological risk index value is calculated for each zone, and the resultant ecological land landscape ecological risk index is assigned to the center point of each evaluation unit. Point data are used as interpolation sample data, and the Kriging spatial interpolation method is applied in ArcGIS to interpolate the ecological risk within WNPSA, resolution is chosen as 650 m, and the landscape ecological risk was interpolated to obtain the spatial distribution of ecological risk. Other landscape structure indices were also analyzed by spatial mapping using a 3 km × 3 km grid to reveal the changing characteristics of landscape ecological structure in WNPSA from multiple perspectives. The calculation formula for the landscape ecological risk index of each assessment unit is as follows:

$$LERI_i = \sum_{x=1}^n \frac{A_i}{A} \times R_i \tag{7}$$

In this context,  $n_i$  denotes the quantity of patches corresponding to landscape type  $i$ , while  $A_i$  signifies the aggregate area of said landscape type. The term  $A$  represents the total area of all landscape types combined, and  $R_i$  represents the ecological land loss degree index.

**Table 1.** Calculation formula of each landscape index and the corresponding ecological significance.

Landscape Index	Calculation Formula	Ecological Significance
Landscape fragmentation index ( $C_i$ )	$C_i = \frac{n_i}{A_i}$ (8)	This value quantifies the extent of fragmentation within a specific ecological landscape type at a specified time and property. The formula is determined by both the total area of the landscape and the number of patches present within that region.
Landscape separation index ( $N_i$ )	$N_i = \frac{A}{2A_i} \sqrt{\frac{n_i}{A}}$ (9)	This value denotes the degree of segregation among various elements or patch individuals within a particular landscape type in ecological land.
Landscape fractal dimension index ( $F_i$ )	$F_i = \frac{2 \ln(\frac{P_i}{4})}{\ln A_i}$ (10)	The variable $P_i$ represents the perimeter of landscape type $i$ within an ecological land. The theoretical range for $F_i$ is established between 1.0 and 2.0, with a higher value of $F_i$ indicative of a more intricate patch shape.
Landscape disturbance index ( $E_i$ )	$E_i = aC_i + bN_i + cF_i$ (11)	In this study, the weights for fragmentation, separation, and fractal dimension are denoted as $a$ , $b$ , and $c$ , respectively, with their sum equal to 1. Drawing upon pertinent literature and expert insights, the fragmentation index was most important, followed by the degree of separation and dominance, the respective weights assigned to these three indicators are determined to be 0.5, 0.3, and 0.2 [53].
Landscape vulnerability index ( $D_i$ )	expert consulting method	The vulnerability index serves as a measure of the resilience of various landscape types within ecological land against external disturbances, thereby reflecting their susceptibility to such disturbances. A higher vulnerability index is indicative of diminished ecosystem stability. We assign a vulnerability index to four distinct landscape types in ecological land—forest, water, shrub, and grassland—based on expert evaluations. These evaluations range from 1 to 4 [54], after which they are normalized.

Table 1. Cont.

Landscape Index	Calculation Formula		Ecological Significance
Vulnerability normalization formula	$Y = \frac{\tan^{-1} x}{\pi}$	(12)	$X = 1, 2, 3, 4$
Landscape loss index	$R_i = E_i \times D_i$	(13)	The Landscape Loss Index quantifies the extent of natural attribute degradation within an ecosystem under both natural and anthropogenic disturbances. This can be articulated by multiplying the disturbance index with the vulnerability index, which is specific to each landscape type.

## 4. Results

### 4.1. Spatiotemporal Evolution of Land Cover in WNPSA

#### 4.1.1. Land Cover Change Analysis

The conversion area between cropland, forest, and impervious surface in WNPSA was large during 1990–2020, mainly including the following: “21 forest → cropland”, “12 cropland → forest”, “18 cropland → impervious surface”, and “28 forest → impervious”, while the change areas of the remaining types are all small (Table 2). In particular, the conversion area of 1990–2000 “12 cropland → forest” was the largest, but after that the area and change rate of cropland to forest conversion decreased gradually. The conversion of “21 forest → cropland” gradually increased, and the change area in 2010–2020 was 145.4 km<sup>2</sup> greater than that in the 1990–2000 period. From 1990 to 2020, the transformation area and change rate of “cropland, forest → impervious surface” continuously increased, indicating that the increase in the area of impervious surfaces in WNPSA was mainly due to the transformation of cropland and forest areas.

Table 2. Change rates and change areas of major land cover change types in WNPSA.

Land Cover Change	1990–2000 Change Rate (Change Area in km <sup>2</sup> )	2000–2010 Change Rate (Change Area in km <sup>2</sup> )	2010–2020 Change Rate (Change Area in km <sup>2</sup> )	1990–2020 Change Rate (Change Area in km <sup>2</sup> )
21 Forest → Cropland	1.2% (148.8)	1.6% (196.8)	2.8% (342.2)	3.9% (466.8)
12 Cropland → Forest	12.3% (152.0)	8.8% (105.8)	5.2% (66.5)	9.3% (115.5)
18 Cropland → Impervious	2.2% (27.6)	1.8% (22.2)	3.7% (46.5)	6.9% (85.3)
28 Forest → Impervious	0.0% (6.0)	0.1% (9.3)	0.2% (20.7)	0.4% (45.6)
15 Cropland → Water	0.3% (3.6)	0.5% (5.6)	0.3% (4.4)	0.9% (11.0)
85 Impervious → Water	3.2% (2.1)	5.8% (5.8)	3.6% (4.6)	11.3% (7.4)
51 Water → Cropland	1.0% (0.5)	2.2% (1.2)	8.0% (4.9)	6.3% (3.1)
25 Forest → Water	0.0% (0.1)	0.0% (0.5)	0.0% (0.3)	0.0% (2.7)
58 Water → Impervious	2.0% (1.0)	1.7% (0.9)	3.1% (1.9)	4.5% (2.2)
42 Grassland → Forest	23.8% (1.3)	14.2% (0.4)	9.4% (0.4)	37.1% (2.1)
52 Water → Forest	3.6% (1.8)	2.0% (1.0)	0.1% (0.0)	4.2% (2.1)
24 Forest → Grassland	0.0% (0.1)	0.0% (0.6)	0.0% (0.6)	0.0% (1.3)
48 Grassland → Impervious	15.5% (0.9)	10.4% (0.3)	37.7% (1.6)	21.1% (1.2)
41 Grassland → Cropland	13.6% (0.8)	21.9% (0.6)	19.6% (0.8)	20.6% (1.2)
81 Impervious → Cropland	0% (0.0)	0.1% (0.1)	0.4% (0.5)	1.7% (1.1)

#### 4.1.2. Land Cover Type Conversion Analysis

Sankey diagrams effectively convey the information contained in cross-tabulation matrices about land cover, offering a visual representation of land cover persistence and its changes across multiple time intervals [55]. In the context of stages (Figure 3), the area that was transferred out of land cover during the period of 1990–2000 was 347.54 km<sup>2</sup>, while the area that was transferred in was 350.58 km<sup>2</sup>. The largest amount of land converted out of cropland was 183.6 km<sup>2</sup>, primarily transitioning into forest, impervious surface, and a minor proportion of water. Forest represented the most significant area transferred in during this period, amounting to 157.74 km<sup>2</sup>, predominantly from cropland. The total

transfer area of land in 2000–2010 was 354.46 km<sup>2</sup>, and the transfer area was 354.41 km<sup>2</sup>, which is basically equivalent to the previous stage. The period with the highest forest exit area was 207.64 km<sup>2</sup>, which mainly changed to cropland, followed by impervious surface and a small amount of water. The highest area of conversion was in cropland, 198.69 km<sup>2</sup>, which was mainly converted from forest. The cumulative out-transfer area and in-transfer area between landmasses amounted to 497.74 km<sup>2</sup> during the period of 2010–2020, marking a significant increase when compared to the preceding two decades. This substantial growth was primarily attributed to the mutual conversion occurring between cropland and forest. Among them, the forest conversion area was as high as 364.16 km<sup>2</sup>, and the cropland conversion area was as high as 348.51 km<sup>2</sup>. In summary, the conversion trajectory of land cover area in different periods from 1990 to 2020 was mainly the flow of cropland, forest, and impervious surface area. The conversion areas of forest continued to decrease, which were 157.74 km<sup>2</sup>, 107.90 km<sup>2</sup> and 67.22 km<sup>2</sup>, respectively, and the conversion area of impervious surface was 70.68 km<sup>2</sup> in 2010–2020, which was significantly increased compared with that of 35.49 km<sup>2</sup> and 32.69 km<sup>2</sup> in the previous two periods.

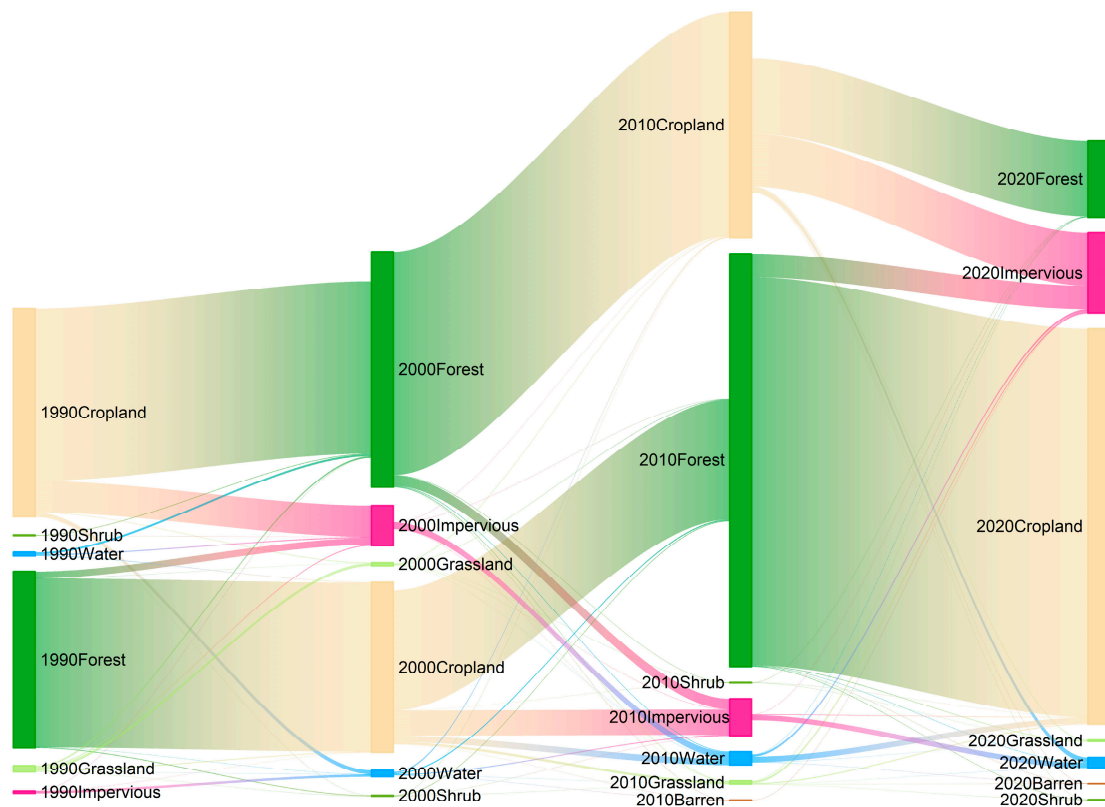


**Figure 3.** Sankey diagram of land cover type transition matrix.

From the perspective of spatial outflow (reduce) and inflow (growth) distribution, the spatial transfer of land cover types was most obvious in cropland and forest during the 1990–2020 period, the spatial distribution range of forest transfer area continuously shrank, the increase area distribution of impervious surface became more concentrated, and the increase area distribution of cropland became increasingly extensive (Figure 4). During the period of 1990–2000, transfer outflow of cropland was most significant in the north of Yanshan County, and the rising inflow of forest was mainly concentrated in the north of Yanshan County as well as in the Guangze County and Jianyang District. The outflow of forests in 2000–2010 had a wide distribution in Wuyishan City, Jianyang District, and Shaowu City, and the rise of croplands corresponded to this area most significantly, impervious surfaces increased significantly and were concentrated in Shaowu City, Jianyang District, and Yanshan County. The outflow of forests in 2010–2020 had a wider range than

the previous two periods, and the inflow of cropland and impervious surfaces were also most obvious, among which the increase in the distribution of impervious surfaces was the most extensive in Jianyang District.

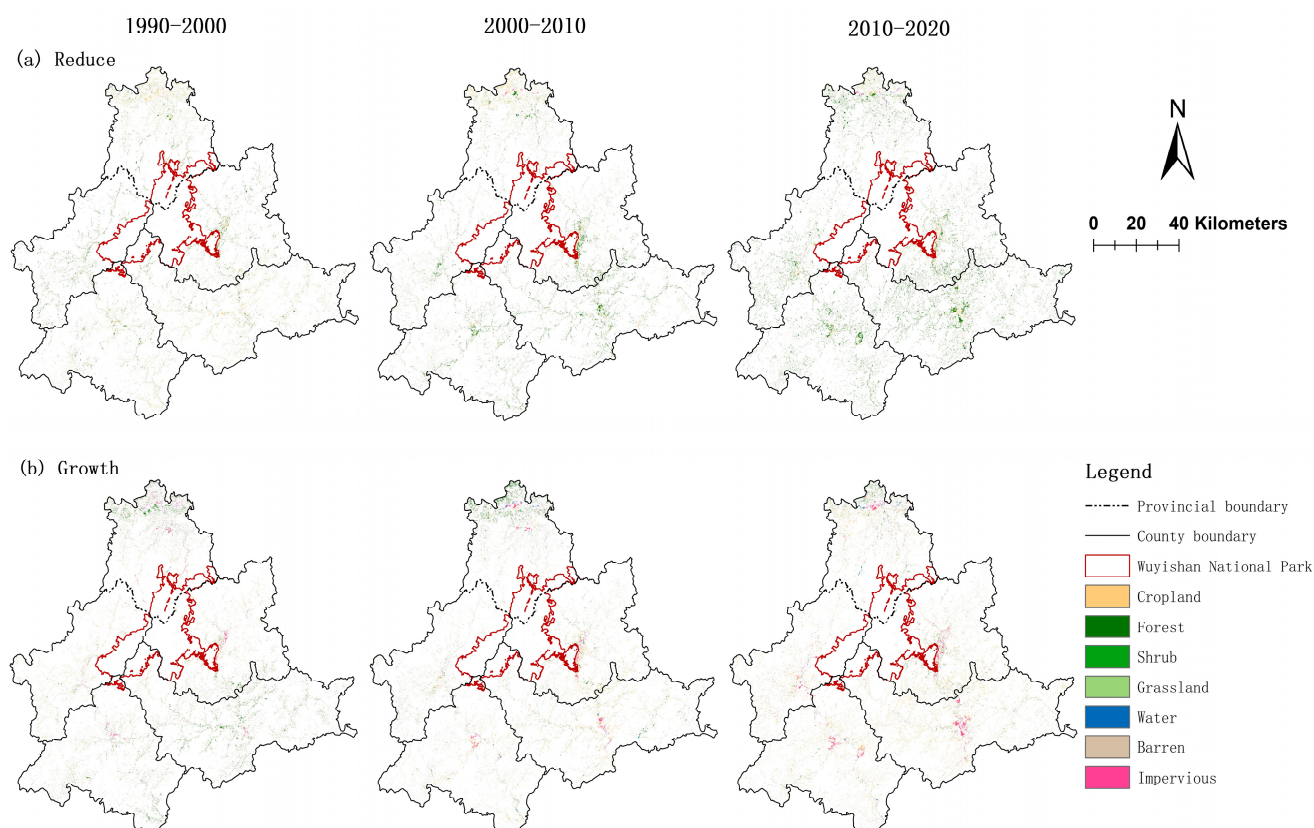


**Figure 4.** Land cover change outflow and inflow profile of WNPSA.

#### 4.1.3. Dynamics of Land Cover Change

Utilizing Formulas (5) and (6), the calculated dynamic degree of each land cover type and the comprehensive land cover passive attitude (Figure 5) found that the difference in the change of dynamic degree of each single land cover type between 1990 and 2020 was significant. The dynamic degree of cropland continued to maintain a positive growth, the comprehensive dynamics were consistent with the changes of impervious surface, and the forest maintained a negative growth in dynamic degree.

Between 1990 and 2000, the comprehensive dynamics were recorded at 0.09%. The single land cover dynamic attitude of impervious surface is the largest, which illustrates that urbanization develops faster in this period, and many lands were exploited as construction land. The forest's dynamics stood at 0.00%, implying that the forested area remained relatively stable. Grassland exhibited the lowest dynamics, signifying a substantial reduction in its area. From 2000 to 2010, the land overall dynamics rose to 0.13%. Cropland dynamics shifted from negative to positive, while forest dynamics declined to  $-0.08\%$ ; this reflects the fact that part of the forest was cleared for agricultural purposes during this period. Impervious surfaces also saw a decrease but maintained a relatively high level. Between 2010 and 2020, the overall dynamics reached 0.18%. Impervious surfaces again emerged as the dominant land cover type, registering a peak at 5.21%, succeeded by cropland which experienced an increase in dynamics to 1.82%. Forest dynamics continued to fall to  $-0.28\%$ . It is illustrated that the population and urbanization of WNPSA are rapidly developing, the forest area continues to decrease, and the area of impervious surface and cropland increases significantly.

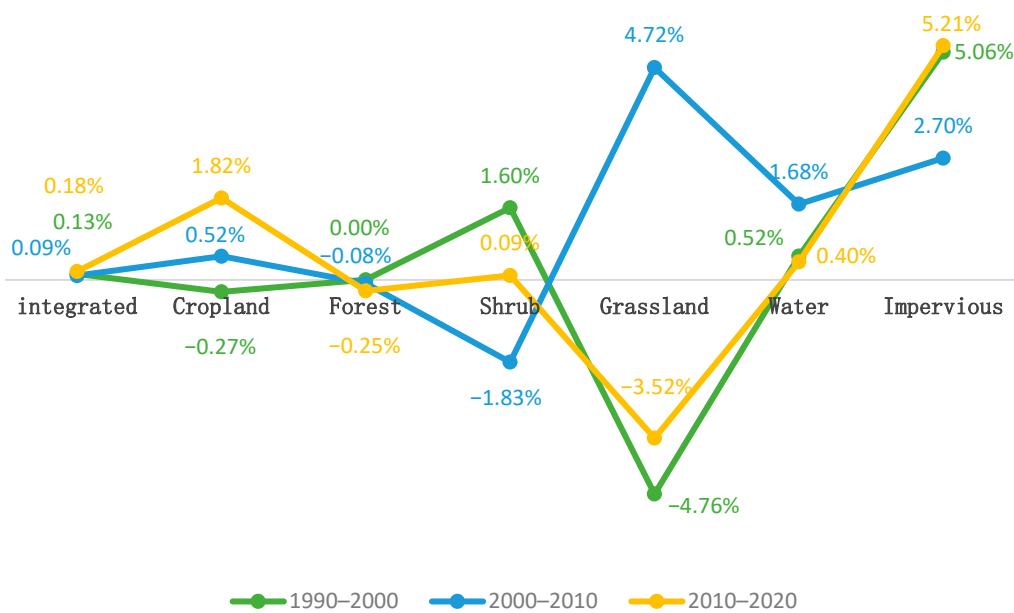


Figure 5. Land cover dynamics change in three periods in WNPSA.

#### 4.1.4. Standard Deviation Ellipse and Centroid Migration Change

Using the metric geographic distribution function analysis of ArcGIS 10.8 software, the standard deviation ellipse of ecological land (including forests, shrubs, grasslands, and water), cropland, and impervious surfaces in WNPSA were plotted for the four time periods from 1990 to 2020, as well as the migratory changes in the centers of gravity (Table 3 and Figure 6).

The standard deviation ellipse and centroid migration changes of ecological land, cropland, and impervious surface in the 30 years from 1990 to 2020 were significantly different. The value gap of the long and short semi-axis of the standard deviation ellipse of impervious surface was the largest, its directionality was the most obvious, the distribution was the most concentrated, and the centroid of the standard deviation ellipse also continued to move southward, reflecting that the development of cities in the south of WNPSA accelerated, and construction land gradually increased. The value gap of the long and short semi-axis of the standard deviation ellipse of cropland was the smallest, closest to a circle, and its directional characteristics were relatively insignificant, so the land cover of cropland was more spatially dispersed than pervious surface and ecological land. The directional changes of the three types were stable, and impervious surface and ecological land always showed a northwest–southeast direction, while cropland always showed a northeast–southwest direction.

In stages, the center of gravity migration of ecological land during 1990–2020 showed a trajectory in the southeast–northwest–southwest direction, the value gap of standard deviation ellipse major and minor semi-axis gradually shortened, and the distribution gradually dispersed. The center of gravity migration of cropland showed a trajectory in the northeast–northwest–southeast direction, the value gap of standard deviation ellipse major and minor semi-axis showed an increasing–increasing–decreasing feature, indicating that the distribution range of cropland showed a trend of concentration during 1990–2010, while the spatial distribution turned to dispersion during 2010–2020. The center of gravity migration trajectory of impervious surface continuously moved southward, the area of standard deviation ellipse continued to increase, and the difference between major and minor semi-axis changed little from 1990–2000 but showed a downward trend during 2000–2010.

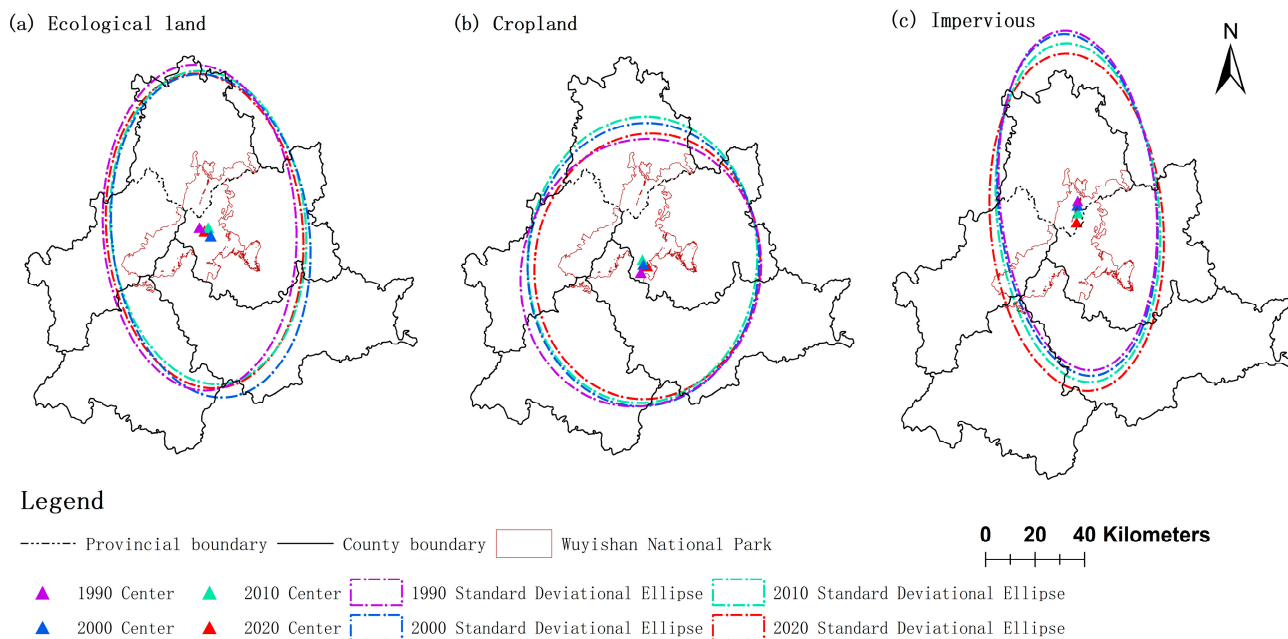


**Figure 6.** Standard deviation ellipses and centroid shifts of ecological land, cropland, and impervious in WNPSA for 1990–2020.

**Table 3.** Ellipse parameters of standard deviation of changes in ecological land, cropland, and impervious in WNPSA for 1990–2020.

<b>Ecological Land</b>	<b>1990</b>	<b>2000</b>	<b>2010</b>	<b>2020</b>
Ellipse x-axis length/km	40.10	40.96	40.45	40.72
Ellipse y-axis/km	67.22	66.86	64.71	65.01
Ellipse area	8467.23	8604.39	8222.64	8316.22
Centroid x-coordinate	117°44'0"	117°46'47"	117°46'10"	117°45'15"
Centroid y-coordinate	27°45'55"	27°44'4"	27°45'53"	27°45'9"
Azimuth (°)	87°6'4"	83°35'53"	85°4'30"	84°46'2"
<b>Cropland</b>	<b>1990</b>	<b>2000</b>	<b>2010</b>	<b>2020</b>
Ellipse x-axis length/km	49.45	47.92	47.58	46.75
Ellipse y-axis/km	55.60	58.53	59.10	54.91
Ellipse area	8637.38	8811.84	8833.77	8063.93
Centroid x-coordinate	117°45'5"	117°45'43"	117°45'29"	117°46'44"
Centroid y-coordinate	27°36'5"	27°37'55"	27°38'58"	27°37'31"
Azimuth (°)	74°56'39"	86°5'53"	86°28'10"	83°49'21"
<b>Impervious</b>	<b>1990</b>	<b>2000</b>	<b>2010</b>	<b>2020</b>
Ellipse x-axis length/km	31.51	31.90	32.87	34.94
Ellipse y-axis/km	68.64	69.08	68.49	68.07
Ellipse area	6794.44	6922.31	70715.32	7471.84
Centroid x-coordinate	117°45'36"	117°45'30"	117°45'37"	117°45'17"
Centroid y-coordinate	27°55'58"	27°55'2"	27°53'2"	27°51'16"
Azimuth (°)	84°25'54"	84°17'47"	84°53'29"	85°11'21"

#### 4.2. Spatiotemporal Variation of Landscape Ecological Risk in WNPSA

##### 4.2.1. Landscape Fragmentation Analysis

Kriging spatial interpolation in ArcGIS and reference to the natural breaks classification were used to rank the landscape fragmentation of ecological land use in WNPSA: lowest-fragmentation area ( $C_i \leq 0.0000027$ ), lower-fragmentation area ( $0.0000027 < C_i \leq 0.0000112$ ), medium-fragmentation area ( $0.0000112 < C_i \leq 0.0000281$ ), higher-fragmentation area ( $0.0000281 < C_i \leq 0.0000535$ ), and highest-fragmentation area ( $0.0000535 < C_i$ ).

The upper landscape fragmentation was low in WNPSA during 1990–2020, with a maximum of 0.00058, but spatial differences were significant (Figure 7). The distribution of lowest-landscape fragmentation dominates within the National Park, and the landscape fragmentation values and spatial patterns do not vary significantly. The high (higher- and highest-) fragmentation areas were concentrated in the northern edge of Yanshan County, Jiangxi Province, but the spatial distribution range continued to decrease over 30 years, and the regional landscape fragmentation decreased, indicating that the integrity and continuity of the ecosystem in this area are constantly improving. In contrast, there is a tendency of medium-fragmentation in the southwest region of Guangze County and the southeast region of Wuyishan City outside the national park. In Fujian Province, a trend of medium- spatial fragmentation was observed in the county town of Guangze, situated near the national park boundary. The landscape fragmentation of Wuyishan City decreased during 1990–2000, but high fragmentation areas appeared during 2000–2020, which may be related to the development and utilization of tourism construction land. The spatial extent of high fragmentation notably increased in the urban area of Jianyang District, which is distant from the national park boundary of WNP. This increase may be attributed to the development and construction of urban built-up areas.

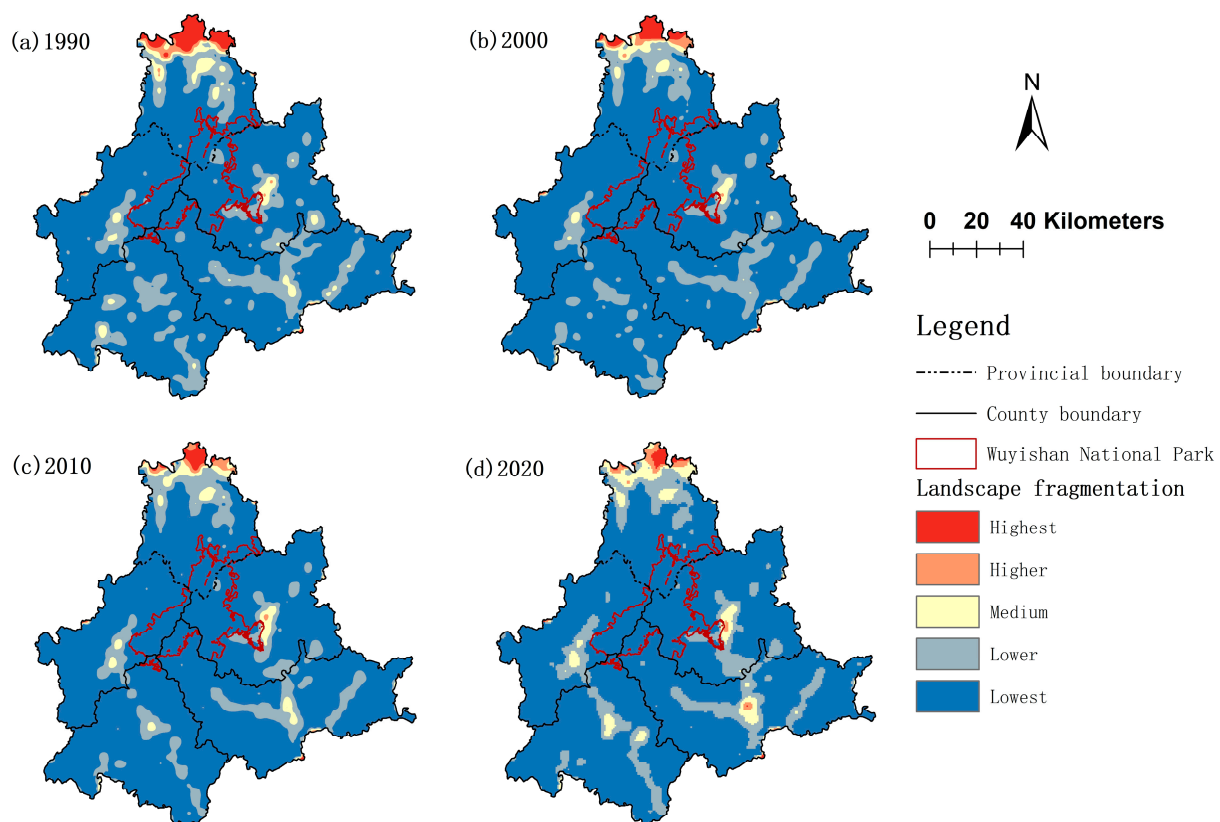
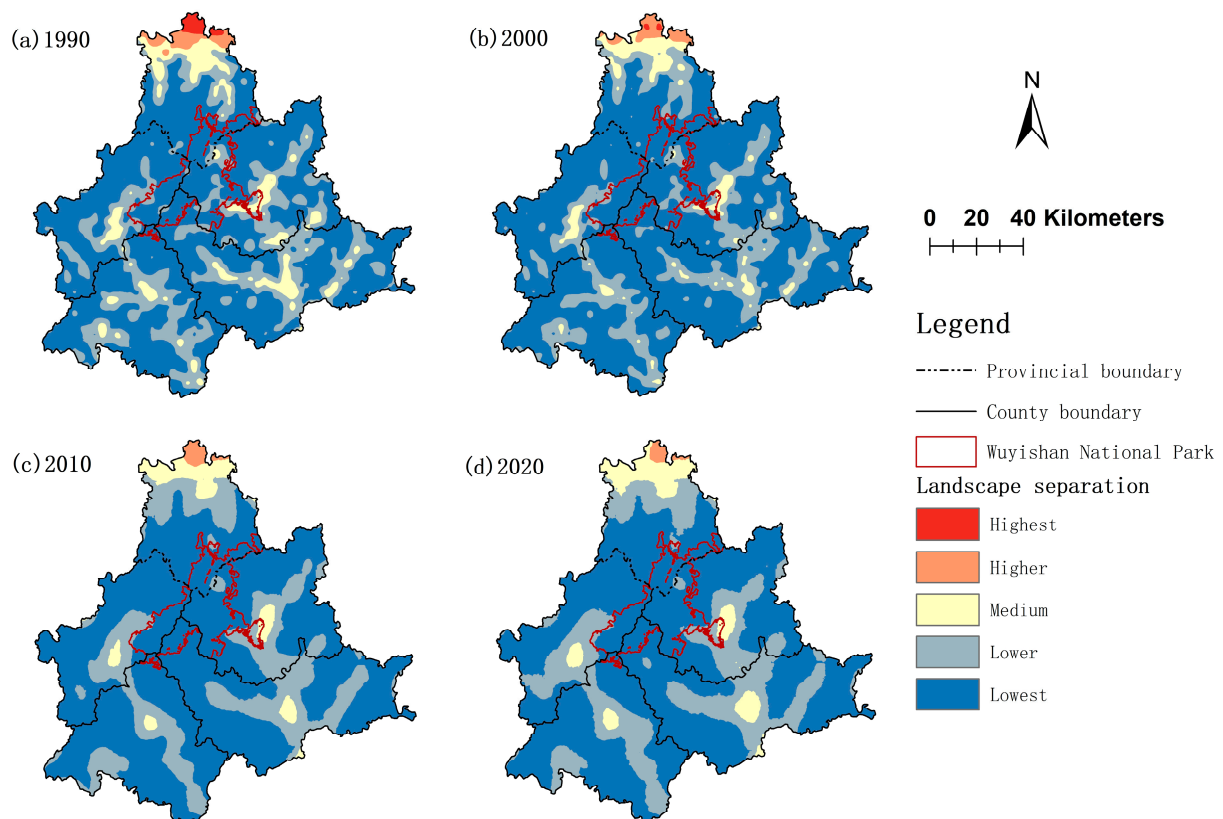


Figure 7. Spatiotemporal changes in landscape fragmentation of ecological land in WNPSA.

#### 4.2.2. Landscape Separation Analysis

Separation analysis offers a precise depiction of dispersed landscape patterns [56]. Kriging spatial interpolation in ArcGIS and reference to the natural breaks classification were used to rank the landscape separation of ecological land use in the study area: lowest-separation area ( $N_i \leq 0.0007$ ), lower-separation area ( $0.0007 < N_i \leq 0.0017$ ), medium-separation area ( $0.0017 < N_i \leq 0.0042$ ), higher-separation area ( $0.0042 < N_i \leq 0.0092$ ), and highest-separation area ( $0.0092 < N_i$ ).

The landscape separation within WNPSA gradually transitioned from dispersed to clustered during 1990–2020 (Figure 8). The highest-separation areas were predominantly located at the northern edge of Yanshan County between 1990 and 2000, subsequently decreasing until they all converged to a lower level of separation. The magnitude of higher-separation areas also diminished gradually, leaving only a minimal range of higher-separation in the northern edge of Yanshan County by 2020. Medium- and lower-separation areas progressively coalesced, with the majority of these areas situated in Yanshan County. The interior of the WNP is primarily characterized by the lowest level of separation, with medium-separation areas persisting at the provincial boundary from 1990 to 2000. However, both medium- and lower-separation areas gradually declined, leaving only minor areas of lower-separation in 2020, and medium-separation was no longer evident.



**Figure 8.** Spatiotemporal changes in landscape separation of ecological land in WNPSA.

#### 4.2.3. Landscape Fractal Dimension Analysis

The fractal dimension index serves as a measure of the shape complexity inherent in landscape patches. A fractal dimension index value closer to 1 indicates a more regular patch shape, thereby increasing the likelihood of disturbance from human activities. Conversely, a value closer to 2 signifies a more complex patch shape and reduces the probability of such disturbances. In this study, the fractal dimension index of ecological landscapes (encompassing forests, shrubs, grasslands, and water) means that the larger the fractal dimension, the more complex the shape of the ecological land patches and

the more they are subjected to anthropogenic disturbances. Kriging spatial interpolation in ArcGIS and reference to the natural breaks classification were used to rank the landscape fractal dimension of ecological land use in WNPSA: lowest-fractal dimension area ( $F_i \leq 1.05$ ), lower-fractal dimension area ( $1.05 < F_i \leq 1.1$ ), medium-fractal dimension area ( $1.1 < F_i \leq 1.15$ ), higher-fractal dimension area ( $1.15 < F_i \leq 1.21$ ), and highest-fractal dimension area ( $1.21 < F_i$ ).

Regions with the lowest-fractal dimensions are predominantly found in WNPSA (Figure 9). A trend of escalating fractal dimension levels is observed from the WNP interior towards its periphery. This can be attributed to the majority of the WNP being forested, ensuring robust landscape integrity and continuity, which results in more regular patch shapes. In contrast, outside of WNP witnesses increasing fragmentation of ecological land due to human activities, culminating in a progressive increase in patch shape complexity. Regions with high-fractal dimensions are primarily located in the most densely populated areas among the five county-level administrative regions, signifying the peak level of human activity. It is worth noting that the highest-fractal dimension of Yanshan county in the Jiangxi part decreased during 1990–2020, while it increased significantly in four administrative districts in the Fujian part, especially in 2020.

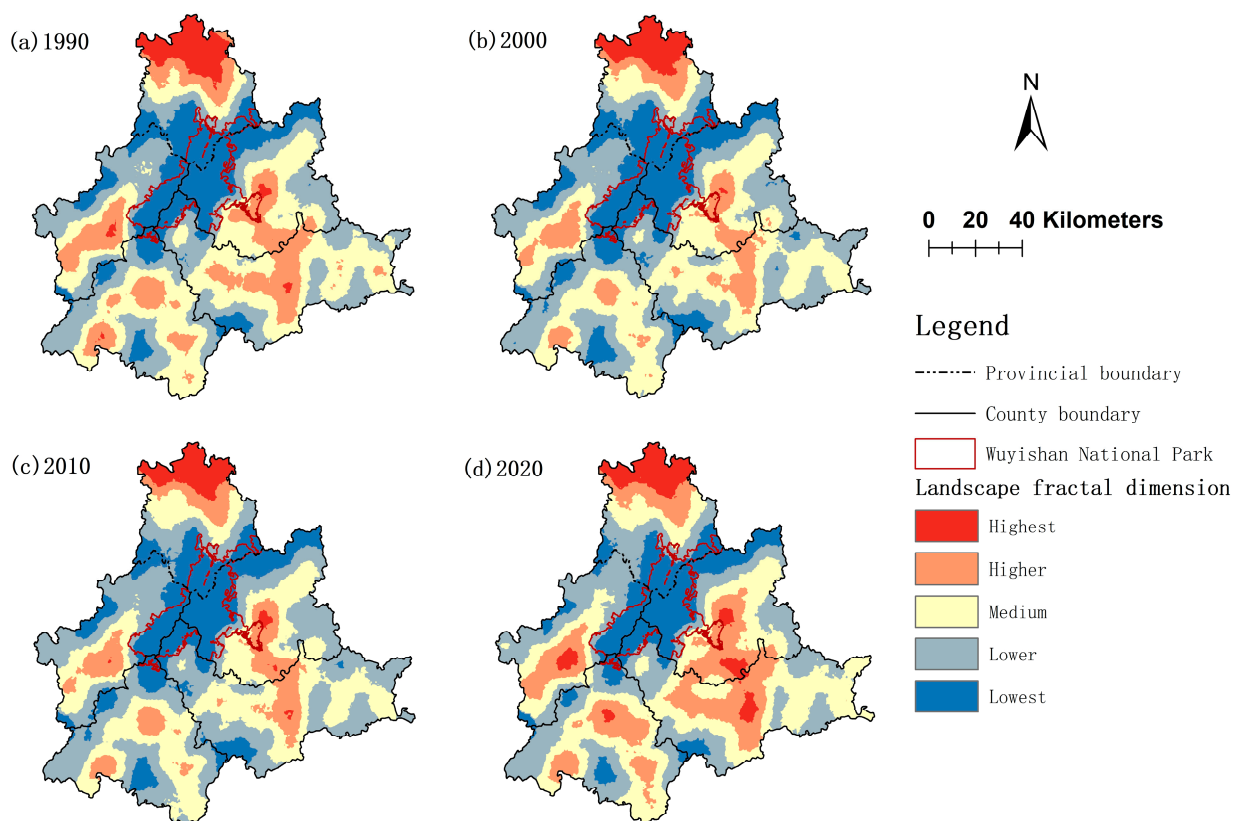


**Figure 9.** Spatiotemporal changes in landscape fractal dimension of ecological land in WNPSA.

#### 4.2.4. Landscape Disturbance Analysis

The landscape disturbance degree of WNPSA was the weighted average of fragmentation, isolation, and fractal dimension (Equation (11)), with the lowest weight for fractal dimension. The pattern of the landscape exhibits significant disparities due to differing degrees of human interference. High levels of human disruption result in increased fragmentation, more intricate patch shapes, diminished connectivity, and heightened diversity [57]. Kriging spatial interpolation in ArcGIS and reference to the natural breaks classification were used to rank the landscape disturbance of ecological land use in WNPSA: lowest-disturbance area ( $E_i \leq 0.21$ ), lower-disturbance area ( $0.21 < E_i \leq 0.22$ ), medium-disturbance

area ( $0.22 < E_i \leq 0.23$ ), higher-disturbance area ( $0.23 < E_i \leq 0.24$ ), and highest-disturbance area ( $0.24 < E_i$ ).

Despite the landscape fractal dimension's weight being the lowest, its influence on disturbance degree is significant due to the small values of fragmentation and separation; the spatiotemporal distribution of landscape disturbance in WNPSA (Figure 10) shows a high similarity with the fractal dimension (Figure 9), while at high values there is a similarity with the distribution of fragmentation and separation. There was a significant downward trend in landscape disturbance degree in 1990–2020 in the northern part of WNPSA in Yanshan County, while the changes in four counties and cities in the southern Fujian Province were more fluctuating, and all of the highest-disturbance areas in 2000 in Guangze County, Shaowu City, and Jianyang District dropped to higher-disturbance areas, and there was also significant shrinkage in high-disturbance areas; by 2010, the highest-disturbance areas appeared again in Guangze County and Wuyishan City. In 2020, medium-, higher-, and highest-disturbance areas in four counties and cities of Fujian Province were more significantly expanded than before.

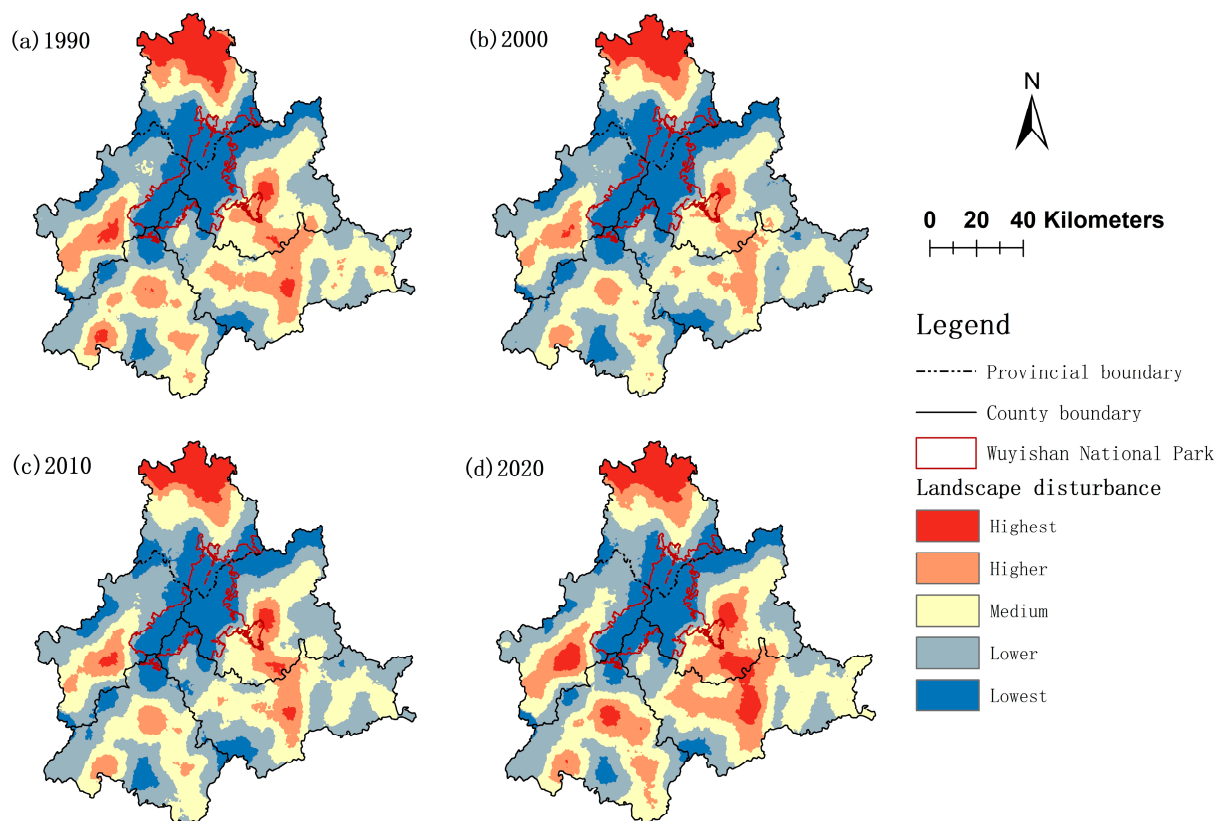


**Figure 10.** Spatiotemporal changes in landscape disturbance of ecological land in WNPSA.

#### 4.2.5. Landscape Vulnerability Analysis

The susceptibility of a landscape pattern is contingent upon both the external influences of human activities and the inherent resilience of the system [58]. Utilizing Formula (12), the normalized vulnerability scores for forest, water, shrubs, and grasslands were ascertained to be 0.5, 0.7048, 0.7952, and 0.8440, respectively. Kriging spatial interpolation in ArcGIS and reference to the natural breaks classification were used to rank the landscape vulnerability of ecological land use in WNPSA: lowest-vulnerability area ( $D_i \leq 0.505$ ), lower-vulnerability area ( $0.505 < D_i \leq 0.53$ ), medium-vulnerability area ( $0.53 < D_i \leq 0.56$ ), higher-vulnerability area ( $0.56 < D_i \leq 0.59$ ), and highest-vulnerability area ( $0.59 < D_i$ ).

The overall ecological land in WNPSA was dominated by low (lower- and the lowest-) vulnerability during 1990–2020, with a higher vulnerability grade corresponding to a

smaller distribution; it can be observed that areas with lower-vulnerability are generally distributed in a strip shape, mainly located along the rivers in WNPSA. Regions with medium- and higher- vulnerability are only found in Yanshan County and Jianyang District, and they are all located between regions of lower-vulnerability (Figure 11). The region with high landscape vulnerability in Yanshan County of Jiangxi Province has significantly shrunk, while the area with medium-landscape vulnerability in Jianyang District of Fujian Province has gradually expanded, and in 2020, a region of higher-landscape vulnerability appeared. In the WNP, there are small areas with lower-vulnerability, which has similarities with the range of fragmentation and separation.

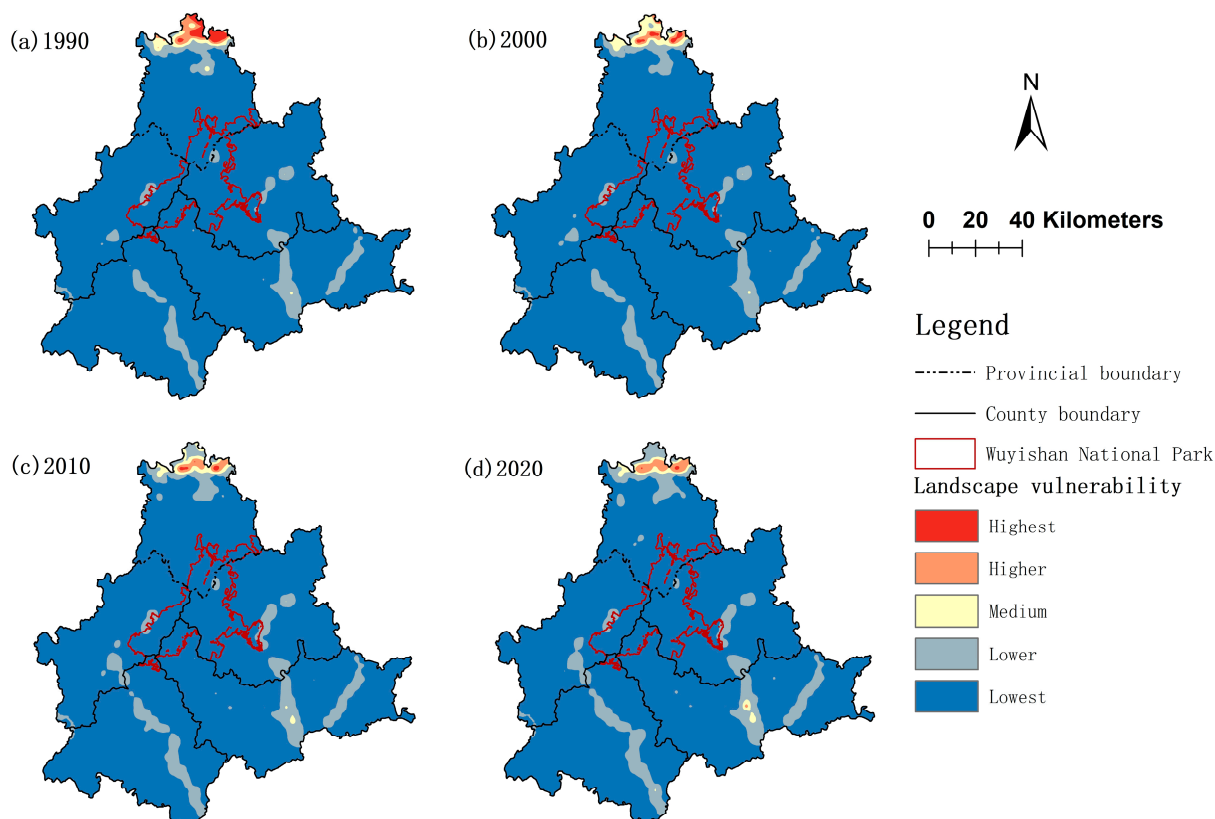


**Figure 11.** Spatiotemporal changes in landscape vulnerability of ecological land in WNPSA.

#### 4.2.6. Spatiotemporal Changes in Landscape Ecological Risk

Kriging spatial interpolation in ArcGIS and reference to the natural breaks classification were used to rank the landscape ecological risk of ecological land use in WNPSA: lowest-risk area ( $LERI \leq 0.105$ ), lower-risk area ( $0.105 < LERI \leq 0.115$ ), medium-risk area ( $0.115 < LERI \leq 0.125$ ), high-risk area ( $0.125 < LERI \leq 0.13$ ), and highest-risk area ( $0.3 < LERI$ ). Changes in the area and proportion of each risk level were calculated for WNPSA and WNP (Table 4).

The spatial pattern of landscape ecological risk between the inside and surrounding areas of WNP during 1990–2020 was significantly different (Figure 12, Table 4). In 1990, the WNP did not contain any high risk zones, and the regions of lower- and medium risk were minimal. These areas of lower-risk predominantly spanned the border regions between Jiangxi and Fujian provinces, as well as the northern and southeastern peripheries of the WNP. By 2000, there was a gradual increase in lowest-risk zones, while the area of lower-risk zones decreased by 2.45% compared to the value in 1990. The area and proportion of medium-risk zones also exhibited a consistent decline. Between 2010 and 2020, all lower-risk zones within the park's northern periphery transitioned into lowest-risk zones at the inter-provincial borders. The lower-risk zone's area dominated the surround-

ing regions of WNP from 1990 to 2020. Meanwhile, the medium-risk zone exhibited a declining trend in 2000 and 2010, followed by an increasing trend in 2020. However, it also experienced significant overall expansion. The highest-risk zone remains confined to the Yanshan County of Jiangxi Province during the past 30 years. The higher-risk zone is predominantly situated in Yanshan County, Jiangxi Province, as well as Wuyishan City and Jianyang District in Fujian Province; the increase in area from 2010–2020 can be seen to be more significant than previous periods. In summary, the area of lower-risk zone in WNP gradually dispersed and narrowed, but there were certain medium-risk zone expansions in the surrounding areas. Specifically, the risk zone in the area adjacent to the southeastern boundary of the WNP has a tendency to expand into the interior of WNP. In addition, the high risk area centered on the county town around WNP will inevitably exert a stress on the ecological corridor in WNPSA. Ecological corridors link the ecological source sites of WNP with those of surrounding areas, covering other nature reserves besides the national park, and these ecological source sites are important for building the ecological base outside the national park and maintaining ecosystem integrity [44].

This study aligned and vectorized the potential ecological corridor [59] in Nanping City, Fujian Province, with the base map of this study to analyze the threat of landscape ecological risk to the ecological corridor in WNPSA. The ecological corridors within the Fujian Province region of WNPSA are predominantly situated in Shaowu City, Wuyishan City, and Jianyang District. The significant expansion of landscape ecological risks with medium and high levels in the region in the surrounding areas of WNP have posed a threat to its ecological corridors and ecological sources (Figure 12), especially the expansion of medium- and higher-risk areas in Wuyishan City and Jianyang District. Such fragmentation may exacerbate the “islanding” phenomenon of national parks, heighten vulnerability, diminish biological protection, and reduce the overall stability of regional ecosystems. Consequently, this could have detrimental effects on surrounding communities and economic development.

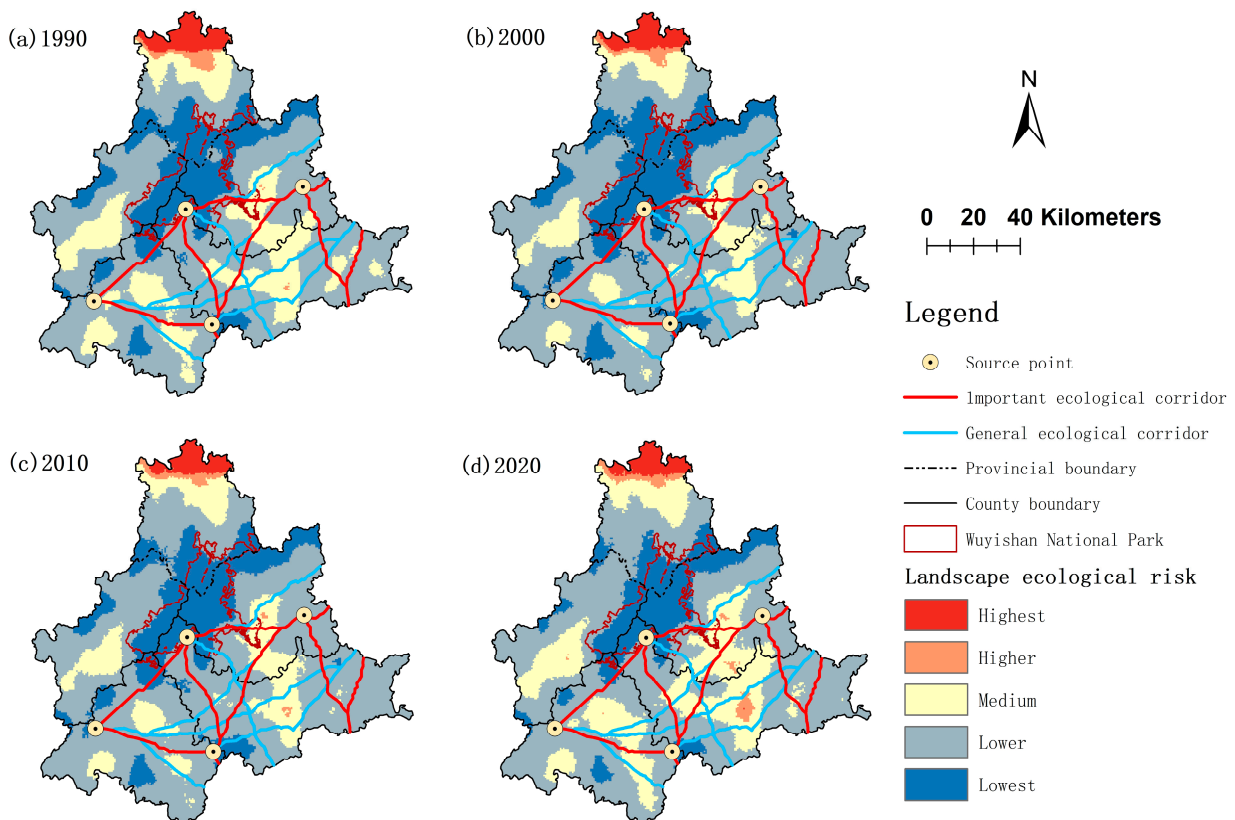


Figure 12. Spatiotemporal changes in landscape ecological risk index of ecological land.

**Table 4.** Area changes of ecological risk levels in WNPSA and WNP.

Time	1990		2000		2010		2020	
	area (km <sup>2</sup> )	Percentage (%)						
WNPSA								
Lowest-risk	2521.90	18.72%	2765.26	20.52%	2654.57	19.70%	2124.75	15.77%
Lower-risk	7744.43	57.47%	8411.98	62.43%	8480.84	62.94%	7722.46	57.31%
Medium-risk	2717.10	20.16%	1877.59	13.93%	1941.81	14.41%	3158.19	23.44%
Higher-risk	145.34	1.08%	113.65	0.84%	127.60	0.95%	200.69	1.49%
Highest-risk	346.03	2.57%	306.31	2.27%	269.98	2.00%	268.71	1.99%
WNP								
Lowest-risk	1009.35	79.13%	1046.96	82.08%	1048.22	82.18%	1048.22	82.18%
Lower-risk	213.36	16.73%	179.56	14.08%	180.83	14.18%	180.83	14.18%
Medium-risk	52.81	4.14%	49.01	3.84%	46.48	3.64%	46.48	3.64%

## 5. Conclusions, Implications and Limitations

### 5.1. Conclusion and Discussion

The land cover in WNPSA from 1990 to 2020 was primarily characterized by the conversion and spatiotemporal variation of cropland, forest, and impervious surface areas, with little conversion and spatiotemporal changes in shrub, grassland, water, and bare lands. The surge in impervious surface area predominantly resulted from the transformation of cropland. Despite a continuous decrease in forest area, the largest conversion occurred to cropland, followed by impervious surfaces. Consequently, the dynamic degree exhibited a consistent negative trend, albeit with a minor value nearing zero. This is attributed to the fact that forests represent the most substantial and expansive land cover type within WNPSA. Although they are on a downward trajectory, the diminished area still constitutes a minor fraction of the total forest area in the region. Both cropland and impervious surfaces witnessed an ongoing increase. In particular, the dynamic for cropland consistently expanded positively. Meanwhile, the dynamic degrees for impervious surfaces and comprehensive dynamic degrees were also positive, exhibiting analogous fluctuation patterns. These levels reached their nadir between 2000 and 2010 and peaked between 2010 and 2020. In the context of spatial distribution, the forest conversion area witnessed a continuous contraction in its range from 1990 to 2020. The center of gravity for ecological land generally shifted southwards, albeit initially moving in one direction before subsequently reversing course. The expansion of impervious surfaces was predominantly observed in the southern section of Fujian Province, with the center of gravity persistently moving further south. This trend indicates that the southern part of WNPSA has continued to increase in urbanization and the overall contraction of ecological land, while the northern part of WNPSA has seen a process of degeneration followed by growth in ecological land. The expansion of cropland became increasingly widespread, lacking distinct directional characteristics, and the migration of the center of gravity remained relatively unremarkable.

The high values of landscape fragmentation, separation, fractal dimension, disturbance, and vulnerability in the landscape ecological structure model all appeared in the county towns of the five counties (cities), followed by areas with more farmland, which were observed in the landscape ecological risk model across five county towns (cities) with a notable increase in areas containing more cropland. In the northern part of WNPSA (i.e., Yanshan County, Jiangxi Province), there are areas with high values of the landscape structure index from 1990 to 2020. However, these zones continued to contract in their spatial range, suggesting an ongoing enhancement in ecosystem integrity and continuity within this region. In contrast, the southern regions (specifically, Fujian Province) displayed a trend towards agglomeration and expansion of higher-value zones. This led to a gradual fragmentation and complexity in the ecological land's landscape shape. In particular, the landscape structure index for the county seat of Guangze County near the national park boundary and Wuyishan City's county town demonstrated an upward trend, extending into the national park's interior. This poses a threat to the national park's ecological security, potentially linked to the expansion of tourist construction land. The spatial range of high

fragmentation in urban areas of Jianyang District, distant from WNP's boundary, expanded due to urban development and construction. Within WNP, the landscape index was predominantly at its lowest grade. High value zones for landscape fragmentation, separation, and vulnerability indices were primarily situated in provincial border areas, with their ranges gradually diminishing. This suggests that the landscape ecological pattern at the junction between Jiangxi Province and Fujian Province remains stable and improving.

The ecological risks associated with the landscape in WNPSA exhibited two distinct trends from 1990 to 2020. The lowest-risk zone was predominantly found within the park itself, while the intersection of Jiangxi Province and Fujian Province was identified as the primary area for shifts in landscape pattern indices and ecological risk aggregation. Despite these changes, the overall landscape ecological risk continued to diminish, alleviating to the lowest-risk zone by 2010. This suggests that land resource development and utilization at provincial junctions necessitate increased cross-provincial cooperation and oversight. This observation aligns with conclusions drawn by researchers examining the ecological security patterns of the Wuyishan national park conservation and development belt. The ecological security level of the WNP is largely high and medium, with only 1.12% of the area exhibiting a low level of ecological security [43]. However, urbanization in nearby counties has amplified and expanded ecological risks. The most notable expansion is observed in the medium- and high-risk zones of Wuyishan City, Jianyang District, and Shaowu City. In particular, the medium-risk zone of Wuyishan City shows a trend towards encroachment into the park. Human activity interference has augmented cropland and impervious surfaces, leading to an increase in fragmented ecological land use and heightening the degree of landscape ecological risk. This has resulted in ecological stress effects on the southeastern edge area of the WNP and regional ecological corridors, intensifying the "islanding" phenomenon in national parks.

## 5.2. Policy Implications

The spatiotemporal variation of land cover and landscape ecological risk in WNPSA has important implications for the synergistic layout of ecological protection in national parks and protected areas around the world:

A regularized mechanism to enhance regional collaborative governance should be established. When a nature reserve spans multiple regions, disparities in management systems, policies, and regulations may arise. These differences can also manifest in resource management and the balance of interests across regions, potentially leading to coordination challenges in governance. Such conflicts can further complicate the utilization of natural resources. WNP, spanning two provinces, exemplifies this issue. By 2010, all landscape ecological risks within WNP had been transformed into the lowest-risk areas, underscoring the efficacy of cross-administrative area collaborative governance. It is imperative to strengthen cross-regional cooperation, establish mechanisms and procedures for collaboration between the two provinces, standardize communication channels, and collectively address ecological risks in national parks and their adjacent areas. This approach offers valuable insights and serves as a reference for governing nature reserves that span multiple administrative regions or even national borders.

Ecological land monitoring, protection and management in national parks and their surrounding areas should be strengthened. The depletion of forests coupled with the expansion of lands and the increase in impervious surfaces has led to landscape fragmentation and separation within the vicinity of national parks, and also amplified the ecological risk associated with these landscapes. Consequently, it is crucial to understand the direction and pattern of land cover transformation, particularly that of ecological land. It is also essential to address the relationship between urban sprawl around national parks and the ecological networks linked to these parks. Furthermore, it is vital to identify the causes of ecological land reduction. Moderate restrictions on urban expansion and agricultural land changes in the surrounding areas of national parks are necessary to mitigate this ecological risk.

The comprehensive protection of ecological corridors within and adjacent to national parks should be strengthened, while simultaneously mitigating the trend of “islanding” within these protected areas. While the landscape continuity and integrity within WNP are commendable, the ecological risk to the surrounding areas of the park was escalating, posing a threat not only to the marginal zones within the park but also to the ecological corridors adjacent to it. To preserve the ecosystem integrity of national parks, it is imperative to prioritize the safeguarding of pivotal ecological corridors in these areas. This requires reducing human disturbance and mitigating damage caused by urban sprawl to these corridors, thereby diminishing the degree of “islanding” of national parks.

### 5.3. Limitations and Prospects

This study analyzes the spatial and temporal evolution of land cover in WNPSA in the four periods from 1990 to 2020 from a regional holistic perspective, and assesses the spatial and temporal changes in landscape ecological risk and its related landscape indices, which is innovative in terms of the research scale and perspectives. However, there are some limitations in this study. Firstly, this paper mainly utilizes the land use cover and its landscape structure to measure the landscape ecological risk without considering the ecosystem service function, and future research can add more ecosystem service index to assess the ecological risk of the whole national park and the surrounding areas. Secondly, due to the limitation of the length of this article, the causes of ecological risk were not examined. The influencing factors of ecological risk can be further explored in future studies by utilizing geographically weighted regression methods and other methods. Finally, this paper discusses the landscape ecological risk of national parks and surrounding areas in the rapidly urbanizing regions of eastern China. In the future, comparative analyses can be conducted on the landscape ecological risk of national parks and surrounding areas in the urban contraction regions of northeastern China and lagging urbanization regions of central and western China, to summarize the evolution of landscape ecological risk under the influence of multi-territory types.

**Author Contributions:** Conceptualization, W.C. and Y.L.; data curation, Y.L.; formal analysis, Y.L. and W.C.; funding acquisition, F.W. and W.C.; investigation, W.C. and Y.L.; methodology, Y.L.; project administration, W.C.; resources, F.W. and Y.L.; supervision, W.C.; validation, Y.L. and W.C.; visualization, Y.L.; writing—original draft, Y.L.; writing—review and editing, W.C. and F.W. All authors have read and agreed to the published version of the manuscript.

**Funding:** This research was funded by Key Program of National Social Science Funds of China “Study on promoting the construction of a protected area system with national parks being the main component” (23AZD062).

**Data Availability Statement:** The data used to support the findings of this study are available from the corresponding author upon request.

**Conflicts of Interest:** The authors declare no conflicts of interest.

## References

1. Zhao, L.; Du, M.; Du, W.; Guo, J.; Liao, Z.; Kang, X.; Liu, Q. Evaluation of the Carbon Sink Capacity of the Proposed Kunlun Mountain National Park. *Int. J. Environ. Res. Public Health* **2022**, *19*, 9887. [[CrossRef](#)] [[PubMed](#)]
2. Li, L.; Tang, H.; Lei, J.; Song, X. Spatial autocorrelation in land use type and ecosystem service value in Hainan Tropical Rain Forest National Park. *Ecol. Indic.* **2022**, *137*, 108727. [[CrossRef](#)]
3. Wescott, G.C. Australia’s distinctive national parks system. *Environ. Conserv.* **1991**, *18*, 331–340. [[CrossRef](#)]
4. Zhu, H.; Liu, J.M. Spatial evolution of the peripheral area of nature reserve under the guidance of tourism: Taking the peripheral area of Changbai Mountain National Nature Reserve as an example. *J. Nat. Resour.* **2023**, *38*, 918–933.
5. Cao, Q.; Zhang, X.; Lei, D.; Guo, L.; Sun, X.; Kong, F.; Wu, J. Multi-scenario simulation of landscape ecological risk probability to facilitate different decision-making preferences. *J. Clean. Prod.* **2019**, *227*, 325–335. [[CrossRef](#)]
6. Xu, J.-Y.; Mao, L.; Zheng, T.-T.; Zhong, Y.-C.; Cehn, G.-L.; Zhang, N. Research on ecological protection planning of surrounding area of national park—A case study of protection and development belt of Wuyishan National Park. *Environ. Ecol.* **2022**, *4*, 31–36.
7. Zheng, Q.M.; Shen, M.Z.; Zhong, L.S. Construction of ecological security pattern in Pudacuo National Park. *Acta Ecol. Sin.* **2021**, *41*, 874–885.

8. Sun, X.; Li, S.; Yu, J.; Fang, Y.; Zhang, Y.; Cao, M. Evaluation of ecosystem service value based on land use scenarios: A case study of Qianjiangyuan National Park pilot. *Biodivers. Sci.* **2019**, *27*, 51–63.
9. Zhang, H.; Han, W.H.; Song, J.Y.; Li, M. Spatial-temporal variations of habitat quality in Qilian Mountain National Park. *Chin. J. Ecol.* **2021**, *40*, 1419–1430.
10. Lin, S.; Hu, X.; Wu, C.; Hong, W. Temporal-spatial features of vegetation cover in Mount Wuyi National Park. *J. For. Environ.* **2020**, *40*, 347–355.
11. Li, J.; Liu, X.; Yao, C.; Gong, H.; Wu, C.; Fan, H. Dynamic change of soil respiration and its effecting factors in different forest lands of Wuyishan National Park. *Acta Ecol. Sin.* **2021**, *41*, 3588–3602.
12. Li, L.C.; Zhou, G.S. Response of forest vegetation to scenic activities in Wuyishan National Park. *Acta Ecol. Sin.* **2020**, *40*, 7267–7276.
13. Tian, Y. Research on Ecological Protection Compensation Mechanism of Shennongjia National Park. Ph.D. Thesis, China University of Geosciences, Wuhan, China, 2021.
14. Dai, Y.C.; Li, D.Q.; Liu, F.; Zhang, Y.G.; Zhang, Y.; Ji, Y.R.; Xue, Y.D. Summary comments on human-bear conflict mitigation measures and implications to Sanjiangyuan National Park. *Acta Ecol. Sin.* **2019**, *39*, 8310–8318.
15. Deng, X.; Wang, Y.; Li, B.; An, T. Poverty issues in a national wildlife reserve in China. *Int. J. Sustain. Dev. World Ecol.* **2010**, *17*, 529–541. [[CrossRef](#)]
16. Wang, M.; Huang, H.; Xiong, J.; Yuan, Z.; Zeng, K. Impact of ecological reserves on the local residents' health: Evidence from a natural experiment in china. *Soc. Sci. Med.* **2023**, *336*, 116186. [[CrossRef](#)] [[PubMed](#)]
17. Xiao, L.L.; Zhong, L.S.; Zhou, R.; Yu, H. Review of international research on national parks as an evolving knowledge domain in recent 30 years. *Prog. Geogr.* **2017**, *36*, 244–255.
18. Zhang, Y.; Sharma, S.; Bista, M.; Li, M. Characterizing changes in land cover and forest fragmentation from multitemporal Landsat observations (1993–2018) in the Dhorpatan Hunting Reserve, Nepal. *J. For. Res.* **2021**, *33*, 159–170. [[CrossRef](#)]
19. Qian, D.; Cao, G.; Du, Y.; Li, Q.; Guo, X. Impacts of climate change and human factors on land cover change in inland mountain protected areas: A case study of the Qilian Mountain National Nature Reserve in China. *Environ. Monit. Assess.* **2019**, *191*, 486. [[CrossRef](#)] [[PubMed](#)]
20. Wang, G.Q.; Song, J.; Xue, B.L.; Xu, X.Y.; Otsuki, K. Land Use and Land Cover Change of Hulun Lake Nature Reserve in Inner Mongolia; China: A Modeling Analysis. *J. Fac. Agric. Kyushu Univ.* **2012**, *57*, 219–225. [[CrossRef](#)]
21. Wan, L.; Zhang, Y.; Zhang, X.; Qi, S.; Na, X. Comparison of land use/land cover change and landscape patterns in Honghe National Nature Reserve and the surrounding Jiansanjiang Region, China. *Ecol. Indic.* **2015**, *51*, 205–214. [[CrossRef](#)]
22. Yu, H.; Zhang, F.; Kung, H.; Johnson, V.C.; Bane, C.S.; Wang, J.; Ren, Y.; Zhang, Y. Analysis of land cover and landscape change patterns in Ebinur Lake Wetland National Nature Reserve, China from 1972 to 2013. *Wetl. Ecol. Manag.* **2017**, *25*, 619–637. [[CrossRef](#)]
23. Recanatesi, F. Variations in land-use/land-cover changes (LULCCs) in a peri-urban Mediterranean nature reserve: The estate of Castelporziano (Central Italy). *Rend. Lincei* **2015**, *26*, 517–526. [[CrossRef](#)]
24. Michel, O.O.; Ying, Y.; Wenyi, F.; Chen, C.; Kaiko, K.S. Examining Land Use/Land Cover Change and Its Prediction Based on a Multilayer Perceptron Markov Approach in the Luki Biosphere Reserve, Democratic Republic of Congo. *Sustainability* **2021**, *13*, 6898. [[CrossRef](#)]
25. Zhang, X.; He, Y.; Zhao, L. The Spatial-Temporal Variation Characteristics of Vegetation Coverage in Five National Parks from 2000 to 2020. *Nat. Prot. Areas* **2023**, *3*, 11–27.
26. Zhang, X.; Ning, X.; Wang, H.; Liu, Y.; Liu, R. Impact of human footprint on landscape fragmentation in the Northeastern China Tiger and Leopard National Park. *Acta Ecol. Sin.* **2022**, *11*, 4688–4702.
27. Li, A.; Ye, C.; Zhu, L.; Wang, Y.; Liang, X.; Zou, Y. Impact from land use/land cover change on function of water yield service: A case study on National Park of Hainan Tropical Rainforest. *Water Resour. Hydropower Eng.* **2022**, *53*, 36–45.
28. Yao, X.; Zhou, L.; Wu, T.; Ren, M. Landscape dynamics and ecological risk of the expressway crossing section in the Hainan Rainforest National Park. *Acta Ecol. Sin.* **2022**, *16*, 6695–6703.
29. Wang, Z.F.; Xu, J. Impacts of land use evolution on ecosystem service value of national parks: Take Sanjiangyuan National Park as an example. *Acta Ecol. Sin.* **2022**, *42*, 6948–6958.
30. Esa, E. Land Use/Land Cover Dynamics and Driving Forces in Simien Mountains National Park, Amhara Region, Ethiopia. *Environ. Sci. Geogr.* **2018**, *5*, 28–43.
31. Hossen, S.; Hossain, M.K.; Uddin, M.F. Land cover and land use change detection by using remote sensing and GIS in Himchari National Park (HNP), Cox's Bazar, Bangladesh. *J. BiNET* **2019**, *2*, 544–554. [[CrossRef](#)]
32. Davidson, I.; O'Shannassy, P. More than just a long paddock: Fostering native vegetation recovery in riverina travelling stock routes and reserves. *Ecol. Manag. Restor.* **2017**, *18*, 4–14. [[CrossRef](#)]
33. Di, F.; Yang, Z.; Liu, X.; Wu, J.; Ma, Z. Estimation on aesthetic value of tourist landscapes in a natural heritage site: Kanas national nature reserve, Xinjiang, china. *Chin. Geogr. Sci.* **2010**, *20*, 59–65. [[CrossRef](#)]
34. Yu, B.; Chao, X.; Zhang, J.; Xu, W.; Ouyang, Z. Effectiveness of nature reserves for natural forests protection in tropical hainan: A 20 year analysis. *Chin. Geogr. Sci.* **2016**, *26*, 208–215. [[CrossRef](#)]
35. Scharsich, V.; Mtata, K.; Hauhs, M.; Lange, H.; Bogner, C. Analysing land cover and land use change in the Matobo National Park and surroundings in Zimbabwe. *Remote Sens. Env.* **2017**, *194*, 278–286. [[CrossRef](#)]

36. Mingarro, M.; Lobo, J.M. European National Parks protect their surroundings but not everywhere: A study using land use/land cover dynamics derived from CORINE Land Cover data. *Land Use Policy* **2023**, *124*, 106434. [[CrossRef](#)]
37. Roy, A. Study of Diversity of Mammals of Rajaji National Park (U.K.) in Relation to Ecoclimatic Changes Due to Anthropogenic Disturbances. *Asian Reson.* **2016**, *1*, 61–66.
38. Singer, F.J.; Zeigenfuss, L.C. *Ecological Evaluation of the Abundance and Effects of Elk Herbivory in Rocky Mountain National Park, Colorado, 1994–1999*; Center for Integrated Data Analytics Wisconsin Science Center: Fort Collins, CO, USA, 2002; pp. 3–55.
39. Bayliss, P.; Dam RA, V.; Bartolo, R.E. Quantitative Ecological Risk Assessment of the Magela Creek Floodplain in Kakadu National Park, Australia: Comparing Point Source Risks from the Ranger Uranium Mine to Diffuse Landscape-Scale Risks. *Hum. Ecol. Risk Assess. Int. J.* **2012**, *18*, 115–151. [[CrossRef](#)]
40. Walden, D.; Bayliss, P. *An Ecological Risk Assessment of the Major Weeds on the Magela Creek Floodplain, Kakadu National Park*; Department of the Environment: Canberra, Australia, 2003.
41. Timko, J.A.; Innes, J.L. Evaluating ecological integrity in national parks: Case studies from Canada and South Africa. *Biol. Conserv.* **2009**, *142*, 676–688. [[CrossRef](#)]
42. Zhang, X.; Yu, H.; Zhang, X.; Zhou, K. Comprehensive evaluation of land ecological security in the Sanjiangyuan National Park based on multi-source data. *Acta Ecol. Sin.* **2022**, *14*, 5665–5676.
43. Yu, Q.Y.; Chen, Y.R.; Wang, L.H.; Yang, B.Y.; Han, X. Spatial-temporal changes of ecological security in Wuyishan National Park and its surrounding areas. *Natl. Park* **2023**, *1*, 116–125.
44. Cui, W.; Wei, Y.; Su, H.; Liu, X.; Wu, D.; Zhang, N.; Ji, N. Research on Ecological Security Pattern Construction of the Protection and Development Belt of Wuyishan National Park. *Res. Environ. Sci.* **2023**, *37*, 874–886.
45. Yang, J.; Huang, X. The 30 m annual land cover datasets and its dynamics in China from 1985 to 2022 [Data set]. *Earth Syst. Sci. Data* **2023**, *13*, 3907–3925. [[CrossRef](#)]
46. Yang, A.M.; Zhu, L.; Chen, S.H.; Jin, H.; Xia, X.X. Geo-informatic spectrum analysis of land use change in the Manas River Basin, China during 1975–2015. *Chin. J. Appl. Ecol.* **2019**, *30*, 3863–3874.
47. Ye, Q.; Liu, G.; Tian, G.; Chen, S.; Huang, C.; Chen, S.; Liu, Q.; Chang, J.; Shi, Y. Geospatial-temporal analysis of land-use changes in the Yellow River Delta during the last 40 years. *Sci. China Ser. D Earth Sci.* **2004**, *47*, 1008–1024. [[CrossRef](#)]
48. Zou, Q.; Zhou, Y.; Li, Q.; Wang, L. Analysis of Spatial Temporal Changes and Trajectory Characteristics of Land Use Pattern in the Southwest Hubei. *J. Soil Water Conserv.* **2022**, *36*, 161–169.
49. Cao, Q.; Zhang, X.; Ma, H.; Wu, J. Review of landscape ecological risk and an assessment framework based on ecological services: ESRISK. *Acta Geogr. Sin.* **2018**, *73*, 843–855.
50. Zhang, W.; Chang, W.J.; Zhu, Z.C.; Hui, Z. Landscape ecological risk assessment of Chinese coastal cities based on land use change. *Appl. Geogr.* **2020**, *117*, 102174. [[CrossRef](#)]
51. Wang, H.; Liu, X.; Zhao, C.; Chang, Y.; Liu, Y.; Zang, F. Spatial-temporal pattern analysis of landscape ecological risk assessment based on land use/land cover change in Baishuijiang National nature reserve in Gansu Province, China. *Ecol. Indic.* **2021**, *124*, 107454. [[CrossRef](#)]
52. Ran, P.; Hu, S. Exploring changes in landscape ecological risk in the Yangtze River Economic Belt from a spatiotemporal perspective. *Ecol. Indic.* **2022**, *137*, 108744. [[CrossRef](#)]
53. Xie, H.-L. Regional eco-risk analysis of based on landscape structure and spatial statistics. *Acta Ecol. Sin.* **2008**, *28*, 5020–5026.
54. Lv, L.; Zhang, J.; Sun, C.Z.; Wang, X.R.; Zheng, D.F. Landscapeecological risk assessment of Xi river Basin based on land-use change. *Ecol. Indic.* **2018**, *38*, 5952–5960.
55. Cuba, N. Research note: Sankey diagrams for visualizing land cover dynamics. *Landsc. Urban Plan.* **2015**, *139*, 163–167. [[CrossRef](#)]
56. Tang, L. The Spatial Pattern Analysis of Landscape and the Landscape Planning in Sheshan Scenic Spot. *Acta Geogr. Sin.* **1998**, *53*, 429–437.
57. Zhou, Y. Spatial and temporal changes of human disturbances and their effects on landscape patterns in the Jiangsu coastal zone, China. *Ecol. Indic.* **2018**, *93*, 111–122. [[CrossRef](#)]
58. Sun, C.Z.; Yan, X.L.; Zhong, J.Q. Evaluation of the landscape patterns vulnerability and analysis of spatial correlation patterns in the lower reaches of Liaohe River Plain. *Acta Ecol. Sin.* **2014**, *34*, 247–257.
59. Xiao, L. Research on Ecosystem Service Function and Network Optimization of Nanping City Based on Ecological Landscape Pattern. Master’s Thesis, Beijing Forestry University, Beijing, China, 2022.

**Disclaimer/Publisher’s Note:** The statements, opinions and data contained in all publications are solely those of the individual author(s) and contributor(s) and not of MDPI and/or the editor(s). MDPI and/or the editor(s) disclaim responsibility for any injury to people or property resulting from any ideas, methods, instructions or products referred to in the content.